Ab Initio Molecular Orbital Study of the Reactivity of Active Alkyl Groups. VII. Solvent Effects on the Formation of Enolate Isomers from 2-Butanone with Methoxide Anion in Methanol

Hirohito IKEDA, Miho YUKAWA, and Tokihiro NIIYA*

Faculty of Pharmaceutical Sciences, Fukuoka University; Nanakuma, Jonan-ku, Fukuoka 814–0180, Japan.
Received November 24, 2005; accepted February 6, 2006

The mechanism of the deprotonation of 2-butanone (1) with methoxide anion (2) was studied by *ab initio* molecular orbital (MO) methods. Calculations of the thermodynamic stabilities of each complex and the regioselectivity of the reaction were performed using a static isodensity surface polarized continuum model (IPCM)[1] which takes the solvent effect into consideration. The calculated energies of the complexes lead ultimately to the conclusion that the major deprotonation pathway in protic solvents is dependent upon thermodynamically stable complexes with small activation energies under equilibrium control.

Key words deprotonation; active alkyl group; *ab initio* molecular orbital (MO) method; enolate; solvent effect

The proton migration in the molecular interaction is a key process in the many chemical and bio-chemical reactions.[2—7] The elucidation of the mechanism of the deprotonation in enzyme-catalyzed reaction is very useful for understanding the mechanism of metabolic reaction.

The deprotonation of an active alkyl compound (AH) by a base catalyst (B^-M^+) is an important first step in various electrophilic substitution reactions. The progress of the deprotonation reaction is expressed in Chart 1. It is well known from regio- and stereoselective studies of enolate formation from ketones that the configurations of enolates are greatly influenced by several factors, *e.g.*, the bulkiness of the carbonyl group substituents, the properties of the base catalysts, the reaction solvent and the temperature of the reaction.[8,9] An important consequence of this is the ability of a ketone to give enolate mixtures of different compositions, depending on whether the enolates were formed under circumstances governed by the relative rates of proton abstraction (kinetic control) or by equilibration of the various enolate anions (equilibrium control).[8]

2-Butanone (**1**) $C^2H_3C^1O^1C^3H_2C^4H_3$ is used as a representative ketone and its deprotonation reactions are summarized in Fig. 1. 2-Butanone (**1**) has two conformations, **1**a and **1**b. The deprotonation of **1**a with **2** $[CH_3O^2]^-$ gives two isomeric products **3**a and **4**a. Also, the deprotonation of **1**b with **2** gives **3**b and **4**b. Under conditions of kinetic control in an aprotic solution, the ratios of the yield of the enolates **3** (**3**a, **3**b), **4**a and **4**b are 5.5, 1.0 and 1.2, respectively.[8] This indicates that the magnitudes of activation energy E_a values of each path in Fig. 1 are path-**3** (path-**3**a and path-**3**b)<path-**4**a≒path-**4**b. Under conditions of equilibrium control in an aprotic solution, the ratio of enolates is **3** (**3**a, **3**b): **4**a : **4**b = 1.0 : 5.3 : 2.0. This indicates that the thermodynamic stabilities of enolates (as M^+ chelated enolates) produced in an aprotic solution are **3** (**3**a, **3**b)<**4**b<**4**a.[8] When the deprotonation proceeds in a protic solvent such as methanol, equilibration between enolate anions and the ketone is achieved rapidly by a large amount of proton donor. It is said that the product yields reflect the thermodynamic behavior of naked or non-chelated enolates.

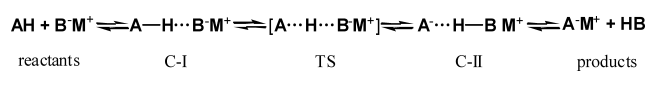

Chart 1

In our previous paper,[10] the deuterium exchange reaction of methyl alkyl ketones was carried out using CH_3ONa in CH_3OD. A linear relationship with a good correlation coefficient (0.97) was obtained between the observed E_a values and the Hartree-Fock E_a values without solvent effects using *ab initio* MO methods. The E_a value for proton abstraction from the methyl group in **1** was smaller than that for proton abstraction from the α-carbon of the ethyl group in **1**. The energy of the optimized geometry of the naked enolate **4**a was higher than that of **3** (**3**a, **3**b). However, under conditions of equilibrium control in methanol, the enolate yields reflect the stability of the enolate anions, *i.e.*, **4**a is more stable than **3**a in protic solvents.[8] Our Hartree–Fock energies of the enolates therefore appear to be in conflict with general theory.

To resolve this conflict and to elucidate the mechanism of the first deprotonation step in electrophilic substitution reactions, the energies of each complex without M^+ chelation were calculated by considering solvent effects and employing Møller–Plesset perturbation theory (MP method) as the elec-

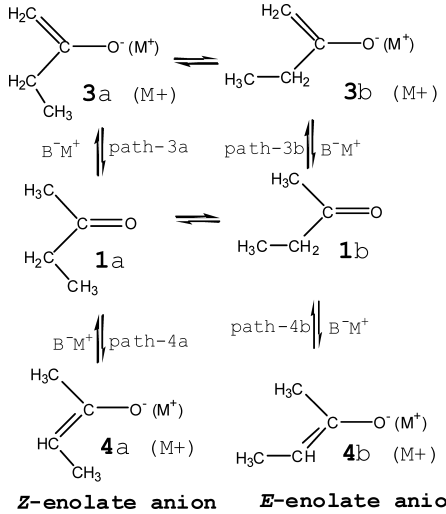

Fig. 1. Path of Deprotonation of **1**a (b) with Base B^-M^+

* To whom correspondence should be addressed. e-mail: niiya@fukuoka-u.ac.jp

tron correlation in MO calculations.[11]

Experimental

Computational Procedures MO calculations were carried out using the Gaussian98[12] and Gaussian03[13] program. The geometries and energies of each complex in the deprotonation of **1** with **2** were calculated using the conventional model where the oxygen atom of **2** approaches the active hydrogen atom of the alkyl group of **1** along the axis of the C–H bond. The most stable conformation of the methoxide fragment in complex was shown in Fig. 2. The optimized geometry in the transition state (TS) was initially determined using HF/6–31+G(d, p) followed by IRC calculations to give complex I (C-I) and complex II (C-II) under solvent-free conditions (Figs. 3, 4). The energies of the solvent-free complexes were calculated with MP3/6–31+G(d, p) level. For the energies of the complexes in CH_3OH, the calculations were performed with a static isodensity surface polarized continuum model (IPCM) using conventional methods, MP3/6–31+G(d, p) level.[11] The value of the dielectric constant ε of methanol for IPCM model is 32.66 at 298 K. The vibrational modes of all transition states were confirmed by frequency analysis.

Results and Discussion

The deprotonation of **1** with **2** is usually carried out in a protic solvent such as an alcohol. It is considered that complexes in methanol exist as the naked (non-chelated) form without a countercation from the base catalyst.

Geometries of Each Complex for Deprotonation of Methyl and Ethyl Groups of 1a with Methoxide The calculated data (optimized geometries and energies) for C-I_a, $TS_{a\text{-}M}$, and C-$II_{a\text{-}M}$ in the deprotonation of the methyl group of **1**a with **2** (path-3a in Fig. 1) under solvent-free conditions were shown in Fig. 3. As the reaction proceeded from C-I_a to C-$II_{a\text{-}M}$ *via* $TS_{a\text{-}M}$, the methoxide anion abstracted an active hydrogen atom from the methyl group of **1**a, rotating about the axis of the C–H bond. The C^1–O^1 bond length then became longer as the $C^2H_3C^1{=}O^1$ moiety changed from a keto type into an enol type. The E_a of path-3a was 4.74 kcal mol^{-1}.

Next, the deprotonation of the ethyl group of **1**a with **2** (path-4a in Fig. 1) was investigated. The geometry of C-I_a in path-4a obtained by the IRC method was the same as in path-3a. The optimized geometries, bond lengths (Å), and energies of C-I_a, $TS_{a\text{-}E}$ and C-$II_{a\text{-}E}$ were shown together with the complexes in path-3a in Fig. 3. The heavy atoms (C^1, C^2, C^3, C^4 and O^1) in C-I_a, $TS_{a\text{-}E}$ and C-$II_{a\text{-}E}$ were located in the same plane. The hybridization of the C^3 atom of the ethyl group changed from sp^3 to sp^2 during the deprotonation process. The other structural changes were similar to those in the case of deprotonation of the methyl group of **1**a. The E_a of path-4a was 4.94 kcal mol^{-1}, and the *Z*-enolate anion was produced.

Geometries of Each Complex for Deprotonation of Methyl and Ethyl Groups of 1b with Methoxide The optimized geometries, bond lengths (Å), and energies of C-I_b, $TS_{b\text{-}M}$ and C-$II_{b\text{-}M}$ for the deprotonation of the methyl group of **1**b with **2** (path-3b in Fig. 1) under solvent-free conditions were shown in Fig. 4. The dihedral angle $\angle C^3C^4C^1C^2$ in C-I_b was twisted about 50 degrees from the carbonyl plane. However, the heavy atoms of the enolate moiety in $TS_{b\text{-}M}$ (and C-$II_{b\text{-}M}$) were located almost in the carbonyl plane. Although the energies of C-I_b, $TS_{b\text{-}M}$ and C-$II_{b\text{-}M}$ in Fig. 4 were higher than those of the corresponding complexes in Fig. 3, the value of E_a (4.87 kcal mol^{-1}) was similar to that of the complex from the methyl group of **1**a.

The optimized geometries, bond lengths (Å), and energies of C-I_b, $TS_{b\text{-}E}$, and C-$II_{b\text{-}E}$ for the deprotonation of the ethyl group of **1**b (path-4b in Fig. 1) under solvent-free conditions were shown in Fig. 4. The structural change from C-I_b to $TS_{b\text{-}E}$ was small, and the position of the C^4 atom deviated

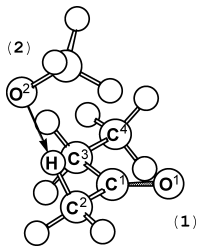

Fig. 2. Initial Geometry for Calculation

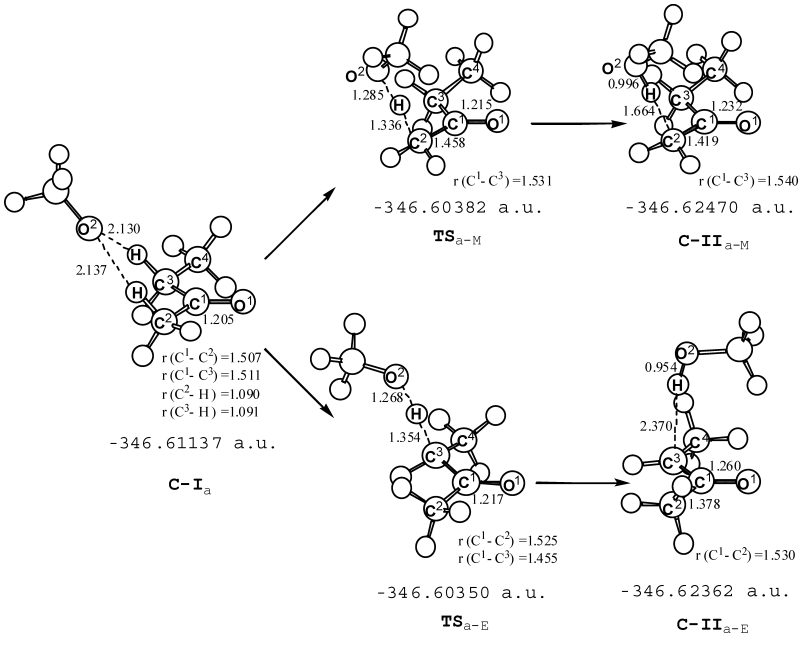

Fig. 3. Deprotonation of Methyl and Ethyl Groups of **1**a with **2**

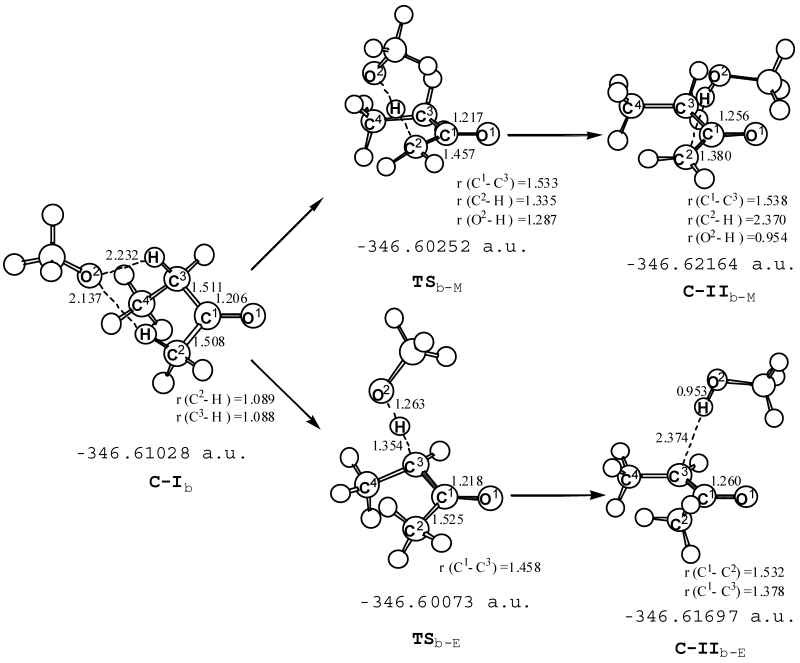

Fig. 4. Deprotonation of Methyl and Ethyl Groups of **1**b with **2**

Table 1. Calculated Energies ($E_{C\text{-}I}$, E_{TS} and $E_{C\text{-}II}$; a.u.) of Complexes and Activation Energies (E_a; kcal) under Solvent-Free Conditions

Compound	Reaction site	$E_{C\text{-}I}$	E_{TS}	$E_{C\text{-}II}$	E_a (kcal)
1a	CH_3	−346.61137	−346.60382	−346.62470	4.74
1a	CH_2CH_3	−346.61137	−346.60350	−346.62362	4.94
1b	CH_3	−346.61028	−346.60252	−346.62164	4.87
1b	CH_2CH_3	−346.61028	−346.60073	−346.61697	5.99

Table 2. Calculated Energies ($E_{C\text{-}I}$, E_{TS} and $E_{C\text{-}II}$; a.u.) of Complexes and Activation Energies (E_a; kcal) in MeOH Using IPCM Model

Compound	Reaction site	$E_{C\text{-}I}$	E_{TS}	$E_{C\text{-}II}$	E_a (kcal)
1a	CH_3	−346.70070	−346.69642	−346.71696	**2.68**
1a	CH_2CH_3	−346.70070	−346.69612	**−346.71852**	2.87
1b	CH_3	−346.69984	−346.69471	−346.71578	3.22
1b	CH_2CH_3	−346.69984	−346.69163	−346.70955	5.15

from the carbonyl plane in C-I_b and $TS_{b\text{-}E}$. The structural changes were similar to those of the deprotonation of the methyl group of **1**b. Again, the heavy atoms of the enolate moiety were in the same plane in C-$II_{b\text{-}E}$, and the *E*-enolate anion was produced.

The energies ($E_{C\text{-}I}$, E_{TS} and $E_{C\text{-}II}$) of each complex and the values of E_a for the proton abstraction of **1** were summarized in Table 1. The energies and E_a values for the deprotonation of the ethyl group of **1**a were all larger than those for the deprotonation of the methyl group. This result indicates that the reaction *via* path-3a proceeds more readily both thermodynamically and kinetically than the other possible reaction paths. However, these calculated results are in conflict with the experimental conclusion[8,9] that the *Z*-enolate **4**a is easily generated under conditions of equilibrium control. If we compare the reactivity of the ethyl group of **1**a and **1**b, the E_a for **1**a is smaller than that for **1**b. It can therefore be concluded that proton abstraction from the ethyl group of **1**a proceeds kinetically. As shown in Fig. 1, the *E*-enolate anion is generated *via* proton abstraction from the ethyl group of **1**b and the *Z*-enolate anion is obtained *via* proton abstraction from **1**a.

Influence of Solvent on the Energies of Each Complex in Deprotonation of 1 with Methoxide Anion in Methanol The IPCM model was used to perform energy calculations in order to resolve the discrepancy between the calculated data under solvent-free conditions and the experimental results.[8,9] Using the optimized solvent-free conformation of each complex (C-I, TS and C-II), the energies of each complex in methanol were calculated with MP3/6–31+G(d, p) level. The calculated results were shown in Table 2. The small value of E_a for path-3a indicates that proton abstraction from the methyl group of **1**a in methanol proceeds kinetically more easily than the other pathways. According to the most stable C-$II_{a\text{-}E}$ in Table 2, we concluded that the *Z*-enolate anion **4**a is thermodynamically generated from **1**a under conditions of

equilibrium control in methanol.

Conclusion

Electrophilic substitution reactions of **1** with **2** are usually carried out in protic solvents such as alcohols. Therefore, MO calculations for the mechanism of the deprotonation step were performed taking the solvent effect into consideration. According to the calculations, the naked enolate anion **3**a was obtained kinetically most easily from **1**a in the deprotonation. The equilibrium between the ketone and the enolate ion was elucidated by the thermodynamic stabilities of the complexes C-I and C-II. It can therefore be concluded that the *Z*-enolate anion **4**a is thermodynamically generated from **1**a under conditions of equilibrium control in methanol.

In conclusion, it is suggested that the IPCM method is useful for understanding the regioselectivity of the deprotonation reaction energetically. The detailed study on the mechanism of this reaction using another solvation model will be reported in the near future.

Acknowledgments The authors thank the Information Technology Center of Fukuoka University for the use of the Fujitsu GP7000S1000 computer, the Computing and Communications Center of Kyushu University for use of the Fujitsu VPP5000/64 computer, and the Research Center for Computational Science at Okazaki National Research Institutes for the use of the NEC SX5 and Fujitsu VPP5000 computers.

References

1) Foresman J. B., Keith T. A., Wiberg K. B., Snoonian J., Frisch M. J., *J. Phys. Chem.*, **100**, 16098—16104 (1996).
2) House H. O., "Modern Synthetic Reactions," 2nd. ed., ed. by House H. O., Benjamin/Cummings Publishing Company, Menlo Park, Calif., 1972, pp. 492—509.
3) Evans D. A., "Assymetric Synthesis," Vol. 3, ed. by Morrison J. D., Academic Press Inc., Orlando, 1984, pp. 2—110.
4) For recent example, see: Murray L. M., O'brien P., Taylor R. J. K., Wünnemann S., *Tetrahedron Lett.*, **45**, 2597—2601 (2004).
5) Colleluori D. M., Reczkowski R. S., Emig F. A., Cama E., Cox J. D., Scolnick L. R., Compher K., Jude K., Han S., Viola R. E., Christianson D. W., Ash D. E., *Arch. Biochem. Biophys.*, **444**, 15—26 (2005).
6) Annedi S. C., Biabani F., Poduch E., Mannargudi B. M., Majumder K., Wei L., Khayat R., Tong L., Kotra L. P., *Bioorg. Med. Chem.*, **14**, 214—236 (2006).
7) Tittmann K., Neef H., Golbik R., Hübner G., Kern D., *Biochemistry*, **44**, 8697—8700 (2005).
8) House H. O., Czuba L. J., Gall M., Olmstead H. D., *J. Org. Chem.*, **34**, 2324—2336 (1969).
9) d'Angelo J., *Tetrahedron*, **32**, 2979—2990 (1976).
10) Niiya T., Yukawa M., Morishita H., Ikeda H., Goto Y., *Chem. Pharm. Bull.*, **39**, 2475—2482 (1991).
11) Foresman J. B., Frisch Æ., "Exploring Chemistry with Electronic Structure Methods," 2nd. ed., Gaussian, Inc., Pittsburgh, PA, 1996.
12) Frisch M. J., Trucks G. W., Schlegel H. B., Scuseria G. E., Robb M. A., Cheeseman J. R., Zakrzewski V. G., Montgomery J. A., Jr., Stratmann R. E., Burant J. C., Dapprich S., Millam J. M., Daniels A. D., Kudin K. N., Strain M. C., Farkas O., Tomasi J., Barone V., Cossi M., Cammi R., Mennucci B., Pomelli C., Adamo C., Clifford S., Ochterski J., Petersson G. A., Ayala P. Y., Cui Q., Morokuma K., Malick D. K., Rabuck A. D., Raghavachari K., Foresman J. B., Cioslowski J., Ortiz J. V., Baboul A. G., Stefanov B. B., Liu G., Liashenko A., Piskorz P., Komaromi I., Gomperts R., Martin R. L., Fox D. J., Keith T., Al-Laham M. A., Peng C. Y., Nanayakkara A., Challacombe M., Gill P. M. W., Johnson B., Chen W., Wong M. W., Andres J. L., Gonzalez C., Head-Gordon M., Replogle E. S., Pople J. A., "Gaussian 98," Revision A.9; Gaussian, Inc., Pittsburgh PA, 1998.
13) Frisch M. J., Trucks G. W., Schlegel H. B., Scuseria G. E., Robb M. A., Cheeseman J. R., Montgomery J. A., Jr., Vreven T., Kudin K. N., Burant J. C., Millam J. M., Iyengar S. S., Tomasi J., Barone V., Mennucci B., Cossi M., Cammi R., Scalmani G., Rega N., Petersson G. A., Nakatsuji H., Hada M., Ehala M., Toyota K., Fukuda R., Hasegawa J., Ishida M., Nakajima T., Honda Y., Kitao O., Nakai H., Klene M., Li X., Knox J. E., Hratchian H. P., Cross J. B., Adamo C., Jaramillo J., Gomperts R., Stratmann R. E., Yazyev O., Austin A. J., Cammi R., Pomelli C., Ochterski J. W., Ayala P. Y., Morokuma K., Voth G. A., Salvador P., Dannenberg J. J., Zakrzewski V. G., Dapprich S., Daniels A. D., Strain M. C., Farkas O., Malick D. K., Rabuck A. D., Raghavachari K., Foresman J. B., Ortiz J. V., Baboul A. G., Clifford S., Cioslowski J., Stefanov B. B., Liu G., Liashenko A., Piskorz P., Komaromi I., Martin R. L., Fox D. J., Keith T., Al-Laham M. A., Peng C. Y., Nanayakkara A., Challacombe M., Gill P. M. W., Johnson B., Chen W., Wong M. W., Gonzalez C., Pople J. A., "Gaussian 03," Revision C.02; Gaussian, Inc., Wallingford CT, 2004.